Quantifying water-use efficiency in plant canopies with varying leaf angle and density distribution

María A. Ponce de León^{a,*}, Brian N. Bailey^a

^aDepartment of Plant Sciences, University of California, Davis, Davis, CA 95616, USA

Abstract

- Background and Aims: Variation in architectural traits related to the spatial and angular distribution of leaf area can have considerable impacts on canopy-scale fluxes contributing to water-use efficiency (WUE). These architectural traits are frequent targets for crop improvement and for improving the understanding and predictions of net ecosystem carbon and water fluxes.
- Methods: A three-dimensional, leaf-resolving model along with a range of virtually generated hypothetical canopies were used to quantify interactions between canopy structure and WUE by examining its response to variation of leaf inclination independent of leaf azimuth, canopy heterogeneity, vegetation density and physiological parameters.
- Key Results: Overall, increasing leaf area index (LAI), increasing the daily-averaged fraction of leaf area projected in the sun direction (G_{avg}) via the leaf inclination or azimuth distribution and increasing homogeneity had a similar effect on canopy-scale daily fluxes contributing to WUE. Increasing any of these parameters tended to increase daily light interception, increase daily net photosynthesis at low LAI and decrease it at high LAI, increase daily transpiration and decrease WUE. Isolated spherical crowns could decrease photosynthesis by ∼60% but increase daily WUE ≤130% relative to a homogeneous canopy with equivalent leaf area density. There was no observed optimum in daily canopy WUE as LAI, leaf angle distribution or heterogeneity was varied. However, when the canopy was dense, a more vertical leaf angle distribution could increase both photosynthesis and WUE simultaneously.
- Conclusions: Variation in leaf angle and density distributions can have
 a substantial impact on canopy-level carbon and water fluxes, with potential trade-offs between the two. These traits might therefore be viable
 target traits for increasing or maintaining crop productivity while using
 less water, and for improvement of simplified models. Increasing canopy
 density or decreasing canopy heterogeneity increases the impact of leaf
 angle on WUE and its dependent processes.

Keywords: Biophysical model, heterogeneous canopies, leaf angle distribution, three-dimensional model, water-use efficiency.

1. Introduction

The potential amount of sunlight that can be intercepted by plants is determined primarily by the angle of leaves relative to incoming beams of solar radiation and by the density and arrangement of neighbouring leaves in space, which is commonly termed canopy structure. The leaf angle can be characterized by the leaf inclination, defined as the angle between the leaf surface normal and the vertical direction, and the leaf azimuthal angle, defined as the polar angle of the projection of the leaf normal on a horizontal plane (Ross, 1981). For a single layer of leaves with no self-shading, the potential light flux that can be absorbed is determined by the fraction of the total leaf area projected in the direction of incoming beams of radiation (Ross, 1981). Neglecting diffuse radiation, a leaf layer with lamina biasing towards a horizontal orientation will intercept more radiation when the sun is near the zenith and less when it is near the horizon (Ehleringer and Werk, 1986; Ezcurra et al., 1991). Adding multiple leaf layers can significantly affect the overall canopy-level behaviour in response to variation in leaf angle (Falster and Westoby, 2003). For example, a canopy with leaves biasing towards the vertical will decrease interception in the upper canopy layers, leading to more transmission of light into the lower canopy and potentially to the ground depending on the overall canopy density (de Wit, 1965).

Absorbed solar radiation drives a wide range of biophysical processes dependent on light or temperature, including photosynthesis, transpiration and metabolism. At the leaf level, the response of photosynthesis to light is highly non-linear. Rates of net photosynthesis tend to increase sharply with increasing light at low light and can be nearly constant or decrease with increasing light at high light (Ort, 2001). The transpiration flux for a leaf typically increases as light increases (Wise et al., 1990), with the slope potentially decreasing because of stomatal closure as radiation-driven temperature increases at high light. The ratio of net photosynthesis to transpiration flux for a leaf, which we term here the water-use efficiency (WUE), tends to increase as light intensity increases and reach an optimum at the point where photosynthesis begins to saturate with light (Kao et al., 1998).

At the canopy level, self-shading attributable to multiple leaf layers can be significant, which can change the emergent whole-canopy-level behaviour of processes related to WUE. Increasing leaf area or having a leaf angle distribution that biases towards the horizontal tends to intercept more light overall, but

Email address: aponcedeleon@ucdavis.edu (María A. Ponce de León)

^{*}Author for correspondence:

can potentially decrease total canopy photosynthetic capacity (Digrado et al., 2020) and WUE owing to excessive shading in the lower canopy (Srinivasan et al., 2017). Canopy architectures with more erect leaves, especially at the top of the canopy, can lead to increased light penetration and an overall increase in canopy photosynthesis and WUE in comparison to horizontally biased leaf angles (Forseth and Ehleringer, 1983; James and Bell, 2000; Long et al., 2006). Although many canopy traits are capable of influencing photosynthesis and WUE, Digrado et al. (2020) found that for cowpea crops, leaf area index (LAI) and leaf area exposure had the largest influence on these processes compared with other traits, such as the number of nodes, stem length and shoot mass.

Understanding the crucial traits underpinning plant WUE is important for a wide range of applications spanning basic biology, agricultural production and plant systems modelling. A primary goal of modern agriculture is to increase or maintain productivity while reducing required inputs, such as water (i.e. higher WUE). This could be accomplished by breeding for cultivars with high photosynthetic capacity (Condon et al., 2004) or by selecting lines with leaves that tend towards the vertical rather than towards the horizontal, which has been done in wheat to increase yields (Richards et al., 2019). For existing cultivars, management practices such as pruning and thinning have been proposed as a means by which WUE can be increased (Forrester et al., 2012; Jin et al., 2018).

Despite the known potential for increasing WUE through variation in plant architectural traits, accurately quantifying or predicting WUE in the presence of many confounding variables has remained a challenge. Our understanding of and ability to measure plant biophysical processes at the leaf level has advanced rapidly owing to portable infrared gas analysers (Long et al., 1996; Watanabe et al., 2005; McPherson, 2007; Song et al., 2013), yet these instruments are low throughput and produce instantaneous measurements for single leaves. Thus, it is difficult to determine how these measurements scale to the canopy level, especially in heterogeneous and anisotropic canopies. Tower-based flux measurements can quantify canopyscale WUE (e.g., Knauer et al., 2018; Nelson et al., 2020), but generally do not allow for systematic variation in structural and physiological parameters because there are usually many confounding covariates when comparing across space and time. Models have been used as an alternative for scaling up leaf-level processes to the canopy level for many decades. However, in traditional land surface models, the canopy is usually represented in these models through simplified equations based on assumptions of horizontal homogeneity and often leaf isotropy (Jones et al., 1991; Humphries and Long, 1995; Lloyd et al., 1995; Foley et al., 1996; Sellers et al., 1996; De Pury and Farquhar, 1997; Jones et al., 2003; Wang and Leuning, 1998). Instead of resolving the fluxes at the leaf level, these simplified models calculate average fluxes for the whole canopy, for horizontal layers of the canopy or for leaf angle classes within layers of the canopy. Thus, there is limited knowledge of the net effect of canopy heterogeneity and anisotropy on these biophysical processes.

High-resolution, three-dimensional (3D) models of plant structure coupled with physically based models of plant function have the capability of realistically representing the 3D arrangement of leaves in space and associated biophys-

ical processes across a wide range of plant canopies with varying levels of leaf anisotropy and heterogeneity. Potential applications are diverse and include energy transfer (e.g., Pearcy and Yang, 1996; Chelle and Andrieu, 1998; Henke and Buck-Sorlin, 2017; Bailey, 2018, 2019), turbulent transport processes (Mahaffee et al., 2023), and photosynthesis (Song et al., 2013; Wang et al., 2017; Bailey and Kent, 2021). Previous work by Le Roux et al. (2001) used a 3D model to study the within-crown variability in WUE in a low-density orchard and found large short-term variation in horizontal WUE gradients within isolated crowns, suggesting potential importance of crown-level canopy structure. However, to our knowledge, 3D models have not been used to study the canopy-scale effect of heterogeneity and anisotropy on WUE.

In this work, we used a detailed 3D leaf-resolving canopy model, Helios (Bailey, 2019), to independently study the effects of interacting plant architectural traits on WUE and related processes. The spatially explicit nature of the 3D, leaf resolving modelling approach allowed for the examination of WUE in response to variation of leaf inclination independent of leaf azimuth, canopy heterogeneity and canopy density (in m² leaf per m³ canopy). We sought to determine cases in which the increase in canopy-absorbed radiation could significantly alter WUE through variation in the distribution of leaf area and angle. To understand the dependence between canopy structure and WUE, we varied parameters driving photosynthesis and transpiration. It was hypothesized that the degree to which leaf angle can affect spatial and temporal variations in WUE is strongly dependent on the spatial distribution and density of leaf area, such that a given leaf angle distribution could either increase or decrease WUE depending on the distribution of leaf area. It was additionally hypothesized that for cases with the same canopy density, the effect of leaf angle variation will increase in heterogeneous canopies.

2. Materials and Methods

2.1. Model description

Leaf-absorbed radiation flux, leaf surface temperature (T_{leaf}) , leaf transpiration flux (E_{leaf}) , and leaf net photosynthetic flux (A_{leaf}) were simulated for a range of homogeneous and heterogeneous canopies using the Helios software (Bailey, 2019). Helios is a 3D plant modelling framework that simulates these biophysical processes at sub-leaf scales such that the entire plant/canopy geometry is fully resolved down to the scale of shadows. The geometry of leaves and the ground surface are represented by a mesh of rectangular patch elements. The model equations described below are applied for every patch element in the simulated domain, then aggregated to determine whole-canopy values (see 'Leaf angle distributions' section). The Helios sub-models used for this study were solar position and incident environmental flux models, radiation transport, surface energy balance, stomatal conductance, and photosynthesis. Each of these sub-models is described in detail in Bailey (2019), and only a brief overview is described below, with details given when specifically relevant to this study.

The solar position/flux sub-model calculates the incoming direct and diffuse solar radiation flux above the canopy using the REST-2 model of Gueymard (2008) and calculates the incoming diffuse longwave radiation flux from the sky using the model of Prata (1996). To calculate the position of the sun and radiative fluxes, this sub-model requires specification of the site longitude, latitude, offset from Universal Coordinated Time (UTC), atmospheric pressure, air temperature (T_{air}) , atmospheric turbidity coefficient, relative humidity (RH), and Julian day of the year.

The radiation transport sub-model calculates the absorbed radiation for every geometric object in the simulated domain and terrestrial emission based on the above-specified ambient radiative fluxes using a reverse ray-tracing approach (Bailey, 2018). For this sub-model, information on surface reflectivity,transmissivity and emissivity of the geometric objects in the simulated domain needs to be specified.

The surface energy balance sub-model calculates the leaf temperature that balances the leaf energy budget equation, which is a balance between energy fluxes of radiation, sensible heat and latent heat (L) as described by Bailey (2019). The net radiative flux for each leaf element was calculated by the radiation transport model as introduced above. The leaf boundary-layer conductance to heat $(g_H, \text{ mol m}^{-2} \text{ s}^{-1})$ was calculated using the Polhausen equation (Schuepp, 1993) as:

$$g_H = (2 \times 0.135) \sqrt{\frac{U}{d}},\tag{1}$$

where U is the wind speed outside of the leaf boundary-layer, d is the characteristic dimension of the leaf, and the factor of 2 accounts for (symmetric) convective heat transfer from both sides of the leaf. The ground boundary-layer conductance was calculated as in the paper by Kustas and Norman (1999):

$$g_H = 0.1662 + 0.4987 \, U. \tag{2}$$

The latent heat flux (in W $\rm m^{-2}$) was calculated for leaf surfaces as:

$$L = \lambda g_w \frac{e_s(T_{leaf}) - e_s(T_{air})RH}{P_{atm}},$$
(3)

where $\lambda=44000~{\rm J~mol^{-1}}$ is the latent heat of vaporization for water, g_w (in mol m⁻² s⁻¹) is the conductance to water vapor from the sub-surface air spaces (i.e., stomatal cavity) to the air outside the surface boundary layer, $e_s(T_{leaf})$ (in kPa) is the saturated water vapor pressure evaluated at the leaf element surface temperature, and $e_s(T_{air})$ (in kPa) is the ambient air saturation vapor pressure.

The value of g_w was calculated, accounting for the serial pathway for water vapor diffusion through the stomata and boundary layer, as:

$$g_w = n_s \frac{\left(\frac{1.08g_H}{2}\right)g_S}{\frac{1.08g_H}{2} + g_S},\tag{4}$$

where the factor 1.08 is based on the higher rate of diffusion of water vapour in the air compared to heat, g_S (in mol m⁻² s⁻¹) is the stomatal conductance to water vapor, and n_s =1 is the number of leaf sides with stomata (i.e., assumed hypostomatous). The stomatal conductance was modelled following Buckley et al. (2012) as:

$$g_S = \frac{E_m(Q_{leaf} + i_0)}{k + bQ_{leaf} + (Q_{leaf} + i_0)D},$$
(5)

where Q_{leaf} (in μ mol m⁻² s⁻¹) is the absorbed leaf photosynthetically active radiation flux and D (in mmol mol⁻¹) is the vapour pressure deficit between the intercellular leaf air spaces and leaf surface. The coefficients E_m , i_0 , k, and b are semi-empirical.

The leaf transpiration flux (in mmol $\rm m^{-2}~s^{-1}$) was calculated from the latent heat term as:

$$E_{leaf} = 1000(L/\lambda). \tag{6}$$

The photosynthesis sub-model calculates the net leaf CO₂ flux, A_{leaf} (in μ mol m⁻² s⁻¹), as the minimum of two potential capacities to fix carbon following the mechanistic biochemical model of Farquhar et al. (1980), expressed as:

$$A_{leaf} = \left(1 - \frac{\Gamma^*}{C_i}\right) \min\left\{W_c, W_j\right\} - R_d,\tag{7}$$

where Γ^* (in μ mol mol⁻¹) is the photosynthetic CO₂ compensation point in the absence of dark respiration, C_i (in μ mol mol⁻¹) is the intercellular CO₂ concentration, W_c (in μ mol m⁻² s⁻¹) is the rate limited by Rubisco, W_j (in μ mol m⁻² s⁻¹) is the rate limited by RuBP regeneration, and R_d (in μ mol m⁻² s⁻¹) is the dark respiration rate.

The values of C_i and A_{leaf} were both calculated in Eq. 7 with the CO₂ diffusion equation $A_{leaf} = 0.75 g_w (C_a - C_i)$, which is solved numerically for C_i using the secant method. The 0.75 factor is based on the lower diffusion of CO₂ in the air compared to water vapor (Campbell and Norman, 1998), and C_a (in μ mol mol⁻¹) is the CO₂ concentration of air outside of the leaf boundary-layer.

The value of W_c was calculated as:

$$W_c = \frac{V_{cmax}C_i}{C_i + K_c(1 + \frac{O}{K_o})},\tag{8}$$

where V_{cmax} (in μ mol m⁻² s⁻¹) is the maximum carboxylation rate, O is oxygen concentration (in μ mol mol⁻¹), K_o (in μ mol mol⁻¹) is the Michaelis-Menten constant for O_2 and K_c (in μ mol mol⁻¹) is the Michaelis-Menten constant for

 CO_2 .

The value of W_j was calculated as:

$$W_j = \frac{JC_i}{4C_i + 8\Gamma^*},\tag{9}$$

with the potential electron transport rate, J (in μ mol m⁻² s⁻¹), calculated as

$$J = \frac{\alpha J_{max} Q_{leaf}}{\alpha Q_{leaf} + J_{max}},\tag{10}$$

where J_{max} (in μ mol m⁻² s⁻¹) is the maximum electron transport rate, and α is a unitless light response rate parameter.

The temperature dependence of Γ^* , K_c , K_o , R_d , V_{cmax} , and J_{max} was included, following the description given by Bernacchi et al. (2001) and Bernacchi et al. (2003) (see also Bailey, 2019, for details on the specific implementation). Helios version 1.2.65 was used to perform the simulations in this work, for which source code can be downloaded from https://www.github.com/PlantSimulationLab/Helios.

2.2. Integration of leaf fluxes

Instantaneous photosynthetically active radiation (PAR) interception for the whole canopy (Q) was calculated from the leaf PAR interception on a per unit ground area basis as:

$$Q = \frac{\sum_{i=1}^{N_l} a_{l,i} Q_{leaf,i}}{a_q},\tag{11}$$

where N_l is the number of leaf elements in the simulated canopy, $a_{l,i}$ is the one-sided surface area of the i^{th} leaf element, and a_g is the total ground surface area occupied by the canopy. The daily integrated Q_c was calculated based on instantaneous values at time step (Δt) up to time n as:

$$Q_c = \sum_{i=1}^n Q_i \Delta t, \tag{12}$$

where Q_i is the instantaneous whole-canopy flux at the i^{th} time step.

Instantaneous WUE for the whole canopy (in μ mol CO₂ (mmol H₂O)⁻¹) was calculated as the ratio of instantaneous whole-canopy fluxes of photosynthesis (A) and instantaneous whole-canopy fluxes of transpiration (E) on a per unit ground area basis as:

$$WUE = A/E, (13)$$

$$A = \sum_{i=1}^{N_l} \frac{a_{l,i} A_{leaf,i}}{a_g},$$
 (14)

$$E = \sum_{i=1}^{N_l} \frac{a_{l,i} E_{leaf,i}}{a_g},\tag{15}$$

where $A_{leaf,i}$ is the net CO₂ flux of the i^{th} leaf element and $E_{leaf,i}$ is the transpiration flux of the i^{th} leaf element.

The daily integrated canopy water-use efficiency (WUE_c) was calculated as the ratio of daily integrated whole-canopy fluxes of A_c and E_c , as:

$$WUE_c = A_c/E_c, (16)$$

$$A_c = \sum_{i=1}^n A_i \Delta t, \tag{17}$$

$$E_c = \sum_{i=1}^n E_i \Delta t, \tag{18}$$

where A_i and E_i are the instantaneous whole-canopy photosynthetic and transpiration fluxes at the i^{th} timestep.

Instantaneous canopy temperature (T_s) was calculated from the patch temperature weighted by patch area for each leaf.

2.3. Weather data

The incoming radiation was calculated based on an assumed virtual site longitude (121.76°W), latitude (38.55°N), offset from UTC (7 h), atmospheric pressure (101 000 Pa), air temperature and humidity (variable), atmospheric turbidity coefficient (0.01) and Julian day of the year (153). The short-wave radiation was assumed to be partitioned between the PAR band (< 700 nm) and the solar near-infrared band (>700 nm), 47 %, and 53 %, respectively. For this study, all solar energy was chosen to be collimated in the direction of the sun, and the sky was assumed to be cloudless. The number of direct rays used to sample each element was 500, and the number of diffuse rays per element was 1000. The radiation transport model recursive scattering depth was chosen to be two (Bailey, 2018).

The air temperature, relative humidity and wind speed were obtained as a 5-min average from the University of California Davis/National Oceanic and Atmospheric Administration (NOAA) local weather station at the Campbell Track in Davis, CA, USA (http://atm.ucdavis.edu/weather/uc-davis-weather-climate-station). During the study period (07:00-19:00 h), the average, maximum, and minimum air temperature was 29.5, 35.4 and 18.8°C, respectively. The average, maximum, and minimum relative humidity was 0.35, 0.18, and 0.64, respectively, and the average wind speed was 3 m s⁻¹.

2.4. Test case set-up

To explore the effect of canopy structure on absorbed radiation, photosynthesis, transpiration and WUE, a range of hypothetical canopies were simulated

with varying levels of leaf anisotropy, canopy heterogeneity and canopy density. Although Helios can represent arbitrarily complex canopy geometries (Bailey, 2019), simplified geometries were chosen for this study in order to isolate various contributors to WUE. Although the canopy cases do not correspond to any particular species, the chosen model input parameters (detailed below) could be thought of as most similar to hypostomatous broad-leafed C3 species.

2.4.1. Leaf and ground parameters

The 3D geometry of the leaves was represented as a 10×10 uniform grid of planar squares, with the total surface area of each leaf being 0.0049 m². It was verified that the chosen leaf resolution was fine enough to resolve shadows (Supplementary Data Figs S1 and S2; Table S1), which is important for accurately determining canopy-scale fluxes (Bailey and Kent, 2021). The canopy height was set to 1 m. The reflectivity of leaves in the PAR band was set to 0.0855, the transmissivity in the PAR band to 0.0428, the reflectivity in the NIR band to 0.4455, and the transmissivity in the NIR band was set to 0.4041 (Ponce de León and Bailey, 2021). The leaf emissivity was assumed to be 0.96 (López et al., 2012). The baseline parameters at 25°C set in the photosynthesis model were $V_{cmax25} = 78.5 \ \mu\text{mol m}^{-2} \ \text{s}^{-1}$, $\alpha = 0.45$, $R_{d25} = 2.12 \ \mu\text{mol m}^{-2} \ \text{s}^{-1}$ and $J_{max25} = 133 \ \mu\text{mol m}^{-2} \ \text{s}^{-1}$. The selected values of V_{cmax25} and J_{max25} are within the range of typical values for native plants (Walker et al., 2014). These parameters were then varied to further explore the dependency between canopy structure and WUE (see Sec. 2.5). The value of V_{cmax25} was systematically varied between 20, 60, and 100 μ mol m⁻² s⁻¹. The corresponding value of J_{max25} for each V_{cmax25} value was calculated according to the empirical relation:

$$\ln(J_{max25}) = a + c \ln(V_{cmax25}), \tag{19}$$

where a was set to 1.01 μ mol m⁻² s⁻¹ and c to 0.89 (Walker et al., 2014). The corresponding value of R_{d25} was calculated for each V_{cmax25} as:

$$R_{d25} = 0.027 V_{cmax25}, (20)$$

where 0.027 is the ratio of R_{d25} to V_{cmax25} for the chosen baseline parameter values.

The stomatal conductance model empirical coefficients i_0 , k, and b were chosen to be equal to the values given by Bailey (2019), which were determined from measurements in *Prunus dulcis* at different combinations of light, temperature, and ambient humidity, where $i_0 = 38.48~\mu\mathrm{mol}~\mathrm{m}^{-2}~\mathrm{s}^{-1}$, $k = 18~383~\mu\mathrm{mol}~\mathrm{m}^{-2}~\mathrm{s}^{-1}$ mmol mol^{-1} , and $b = 49.68~\mathrm{mmol}~\mathrm{mol}^{-1}$. A value of E_m of 10 mmol $\mathrm{m}^{-2}~\mathrm{s}^{-1}$ was chosen as the baseline value, and E_m of 20.4 mmol $\mathrm{m}^{-2}~\mathrm{s}^{-1}$, which was measured by Bailey (2019), was also included in the study (see Sec. 2.5).

The ground surface was represented as a 20×20 grid of rectangular patches. For all cases, periodic boundary conditions were applied in the horizontal directions to yield a horizontally infinite canopy. For the ground, the energy balance was applied by assuming no latent cooling attributable to water evaporation from the soil, and the heat storage term parameters were chosen as in the study

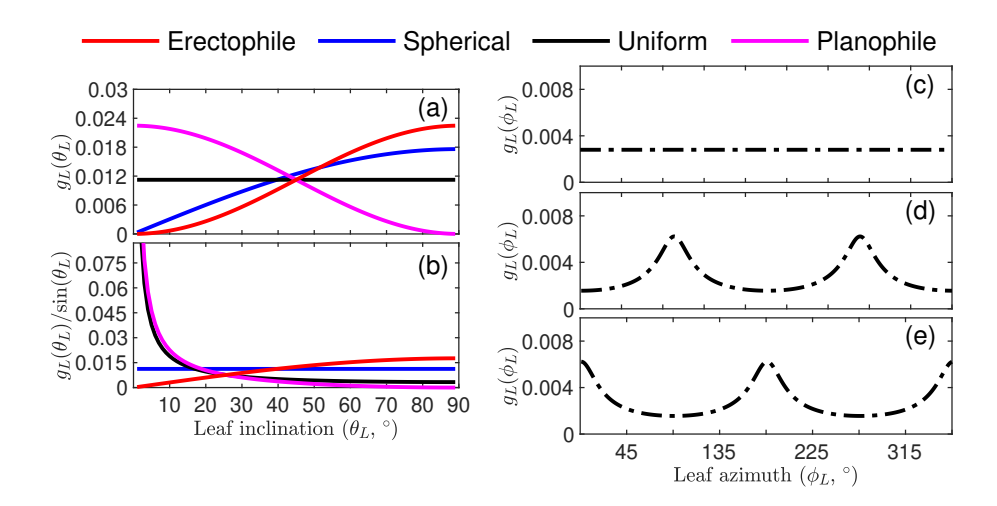


Figure 1: Probability density function of (a) sine-weighted and (b) actual leaf inclination angle for canopy configuration cases with different distributions: spherical, uniform, planophile, and erectophile and of different leaf azimuth: (c) isotropic, (d) leaves biased toward N-S and (e) leaves oriented E-W. Each solid line corresponds to a different leaf inclination angle distribution and each dashed line to a different leaf azimuth distribution. To more clearly depict differences among the actual leaf inclination angles, the y-axis was truncated in (b).

by Ponce de León and Bailey (2021). For simplicity, the ground was considered to be black.

2.4.2. Leaf angle distributions

Hypothetical canopies were generated with varying leaf inclination and azimuth distributions. The leaf inclination distributions $g_L(\theta_L)$ were generated by randomly sampling leaf angle inclinations from four different archetypal leaf angle distributions proposed by de Wit (1965) using the mathematical definitions of Goel and Strebel (1984) (Fig. 1a): spherical (isotropic); uniform (moderately biasing towards horizontal leaves); planophile (strongly biasing towards horizontal leaves), and erectophile (moderately biasing towards vertical leaves).

There is often confusion regarding these classical leaf angle distributions owing to the fact that their definitions usually include a pre-weighting of the leaf angle distribution by solid angle (i.e., multiplication by $\sin \theta_L$, where θ_L is the leaf inclination angle). This weighting by solid angle is necessary when integrating the probability distribution over θ_L in a spherical coordinate system. However, the unweighted probability density is given by $g_L(\theta_L)/\sin \theta_L$, which is plotted in Fig. 1b. Using this normalization, the expected isotropic distribution for "spherical" leaves is achieved (i.e., constant probability with respect to θ_L). It can also be seen that the planophile distribution is much more strongly biased towards horizontal leaves than is the erectophile distribution towards vertical leaves. For reference, the fraction of leaf area projected in the vertical direction [G(0); Ross (1981)] is G(0) = 0.85 for the planophile

distribution and G(0) = 0.42 for the erectophile distribution, illustrating quantitatively that the planophile distribution is much further from the spherical distribution (G = 0.5) than the erectophile distribution. Figure 1b also shows that the so-called uniform distribution is significantly biased toward horizontal leaves [G(0) = 0.64].

For each configuration, the leaf azimuth angles were sampled from a uniform distribution (azimuthally isotropic) independently of leaf inclination, and two contrasting anisotropic leaf azimuth distributions in which leaves were biased towards either the north–south (N–S) or east–west (E–W) directions. Note that in the spherical coordinate system, each azimuthal angle has the same solid angle and thus there is no confusion with regard to solid angle weighting when integrating. Biasing leaves towards horizontal considerably increases the fraction of leaf area projected in the direction of the sun, G, relative to the spherical case (G(0) = 0.5) throughout most of the day and might reduce it in the early and late daylight hours. The opposite is true for the vertically biased distribution (erectophile). Biasing leaf azimuth towards the E–W directions tends to increase G in the early and late hours of the day, whereas the N–S distribution has the opposite effect.

2.4.3. Case 1: homogeneous canopy

A set of homogeneous canopies were created with uniformly distributed leaves in space and varying leaf orientation distribution and LAI values. The number of leaves in the canopy was chosen to achieve four different LAI values: $0.5,\,1,\,3$ and 5. The horizontal extent of the homogeneous canopy was $5~{\rm m}~\times~5~{\rm m}$ (but was extended infinitely through a periodic boundary condition). Homogeneous canopy geometries were generated for all combinations of the four LAI values and all leaf angle distribution cases described above (48 total cases). A sample visualization of the 3D distribution of modelled WUE for the homogeneous canopy case with spherical leaf inclination distribution and isotropic leaf azimuth is shown in Fig. 2a.

2.4.4. Case 2: heterogeneous canopy

Heterogeneous canopies were composed of spherical crowns filled with homogeneous vegetation arranged in a N–S row orientation and with three different row spacings: 1, 2 and 3 m. For all the cases, the spherical crowns had the same leaf area density of 5 m² m⁻³, but different canopy-level LAI attributable to the varying row spacing; 2.6 m² m⁻² for 1 m row spacing, 1.3 m² m⁻² for 2 m row spacing and 0.9 m² m⁻² for 3 m row spacing. The radius of the spherical crowns was 0.5 m, the crown spacing within each row was 1 m and there were 12 spherical crowns explicitly represented in total (but with periodic boundary conditions). The set-up of leaf inclination angle distribution was the same as case 1 (Fig. 1). The horizontal extent of the heterogeneous canopy varied based on the row spacing: for 1 m row spacing, 4 m \times 3 m; for 2 m row spacing, 8 m \times 3 m; and for 3 m row spacing, 12 m \times 3 m. A sample visualization of the 3D distribution of WUE for the heterogeneous canopy case with 2 m row spacing and spherical leaf inclination distribution is shown in Fig. 2b.

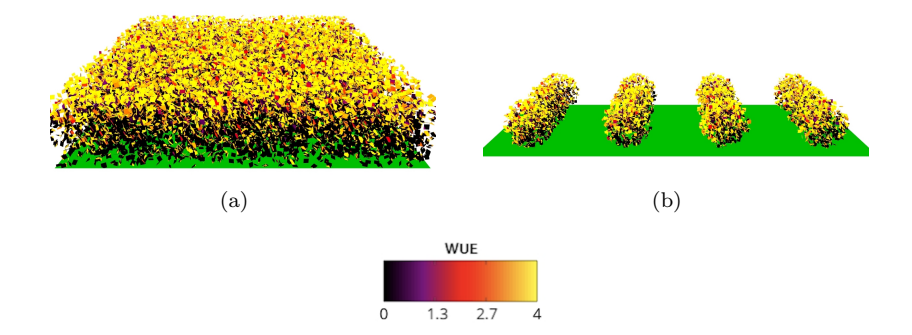


Figure 2: Three-dimensional visualization of the canopy water use efficiency (WUE, μ mol CO₂ (mmol H₂O)⁻¹) at 10:00 hours for: (a) homogeneous canopy case (LAI of 5) and (b) heterogeneous canopy with 2-m row spacing, each with isotropic leaf inclination and azimuth distribution. Each leaf element is colored based on a pseudocolor mapping between its calculated WUE and the color scale shown in the figure. The ground was colored green for contrast, as its WUE was undefined (A = E = 0). The canopies shown all had a leaf area density of 5 m² m⁻³.

2.5. Analysis of physiological parameters

To determine whether the effect of leaf angle varies owing to changes in leaf physiological parameters and to explore further the dependence between canopy density and WUE, parameters driving photosynthesis and transpiration were varied. For the analysis, V_{cmax25} was varied from 78.5 (reference) to 20, 60 and 100 μ mol m⁻² s⁻¹, R_{d25} was varied as a function of V_{cmax25} according to Eq. 20 from 2.1 (reference) to 0.5, 1.6, and 2.7 μ mol m⁻² s⁻¹, J_{max25} was varied as a function of V_{cmax} according to Eq. 19 from 133 (reference) to 39.5, 105 and 165 μ mol m⁻² s⁻¹. Furthermore, parameter values of α were varied from 0.45 (reference) to 0.27 and 0.135 and values of E_m were varied from 10 (reference) to 6.2, 12.3, and 20.4 mmol m⁻² s⁻¹. This analysis considered a subset of the homogeneous canopy cases that included different LAI values (0.5, 1, 3 and 5), with four different leaf angle distributions (spherical, uniform, planophile and erectophile, each with isotropic leaf azimuth).

3. Results

3.1. Case 1: homogeneous canopy

3.1.1. Effect of leaf inclination distribution and LAI in a homogeneous canopy As expected, daily PAR interception increased logarithmically as LAI was increased, with a diminishing rate of increase in Q_c as LAI increased. As the leaf angle distribution was increasingly biased towards horizontal leaves, the daily-averaged value of G_{avg} increased (Fig. 3a,d), which increased daily PAR interception (Fig. 4a). The effect of G on PAR interception at any instant during the day is relatively large, whereas the effect of G_{avg} on daily integrated PAR interception was comparatively small. The impact of leaf angle on Q_c diminished

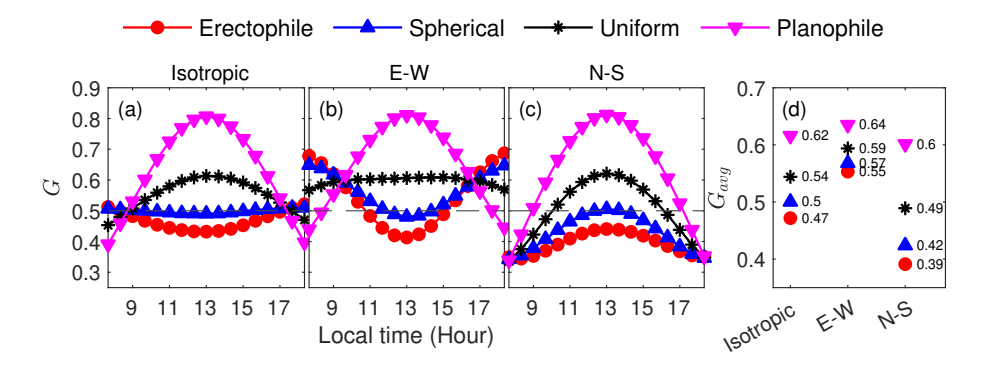


Figure 3: Fraction of leaf area projected in the direction of the sun, G, for the virtual canopies with four different leaf inclination distributions (erectophile, spherical, uniform, and planophile) and three different leaf azimuth distributions (isotropic, leaves biased toward E-W, and leaves biased toward N-S). (a-c) Instantaneous G, and (d) daily averaged G (denoted as G_{avg}). The different line symbols correspond to leaf inclination distributions; sub-plots (a-c) correspond to leaf azimuth distributions.

as LAI increased. There was a 28% difference in Q_c between the erectophile and planophile leaf angle distributions when LAI = 0.5, which decreased to \sim 4% when LAI = 5 (Fig. 4e). This is attributable to the fact that at high LAI, PAR absorption by the canopy approaches 100% regardless of the value of G.

Although Q_c increased monotonically with LAI and G_{avg} , the trend in daily canopy photosynthesis, A_c , reversed as the canopy transitioned from low to high LAI (Fig. 4b). Below an LAI of approximately three, A_c increased as LAI increased and increased as G_{avg} increased (increasing bias towards horizontal leaves). Above an LAI of around three, A_c decreased as LAI or G_{avg} was increased, with the sensitivity of A_c to G_{avg} increasing as LAI increased (Fig. 4f). At low LAI, A_c is limited by the ability to capture light that would otherwise be lost to the ground, and thus higher LAI and Q_c increases daily photosynthesis in this regime. When the canopy is nearly optically thick at high LAI and little light is lost to the ground, A_c is limited by shaded leaf area. As LAI becomes large, shaded leaf area becomes the majority fraction, which has small or negative net photosynthetic fluxes owing to respiration. If the additional photosynthetic productivity of sunlit leaf area attributable to a marginal increase in LAI is less than the respiratory costs associated with shaded leaf area owing to the same increase in LAI, overall canopy photosynthesis will decrease. For the simulation parameters chosen here, this appears to occur for LAI $\gtrsim 3$.

Although LAI has a minimal impact on the photosynthetic flux of sunlit leaf area, G determines the average direct PAR flux on sunlit leaf area and thus determines the photosynthetic flux on sunlit leaf area. The response of leaf photosynthesis to light is logarithmic, meaning that the largest gains in photosynthesis from an increase in light are at lower light. When LAI is small, increasing G increases PAR intercepted by the canopy, which increases A_c . However, when LAI is large, increasing G increases the average PAR flux on sunlit

leaves, which will increase leaf photosynthesis (assuming that the increase in PAR does not cause an excessive temperature increase that decreases photosynthesis) and also increases the fraction of shaded leaf area. If the respiratory costs associated with increased shaded leaf area outweigh the increases in photosynthesis owing to increased sunlit PAR flux, photosynthesis can decrease as G is increased.

The increase in daily canopy transpiration, E_c , with increasing LAI was nearly linear as the LAI increased from 0.5 to 5, with relatively close correspondence between E_c and Q_c (Fig. 4a,c). The effect of the leaf angle distribution via G_{avg} was relatively minimal ($\lesssim 10\%$ between erectophile and planophile distributions), and its effect was non-monotonic as LAI was varied (Fig. 4g). At low LAI, increasing G_{avg} increased E_c , whereas the opposite was true at the highest LAI of five. This appears to be attributable to the fact that the leaf angle distribution has an opposite effect on sunlit vs. shaded leaf area. At low LAI, increasing G_{avq} increases light capture by the canopy, which increases transpiration. At high LAI, there is a marginal increase in additional light capture when LAI is increased, and most additional leaf area added is shaded. Once the canopy is nearly optically thick, varying G_{avg} primarily affects the vertical distribution of energy rather than whole-canopy energy capture. Thus, increasing G_{avg} at high LAI tends to decrease E_c by concentrating energy in the upper canopy. However, sunlit and shaded leaf area both contribute positively to E_c . Thus, an optimum in E_c with respect to LAI does not occur.

Although the effect of LAI on A_c and G_{avg} on A_c and E_c was non-monotonic, the effect of both LAI and G_{avg} on daily canopy WUE was monotonic. The decrease in WUE_c with increasing LAI was nearly linear (Fig. 4d). Increasing G_{avg} tended to decrease WUE_c , with this effect being negligible at an LAI of 0.5, and causing $\sim 35\%$ change in WUE_c between the erectophile and planophile canopies at LAI = 5 (Fig. 4h).

The instantaneous whole-canopy fluxes of Q tended to follow the magnitude of the incoming radiation flux, and the effect of the leaf angle distribution closely followed the diurnal trend in G (Figs. 3a and 5). Similar to the increase in Q, A increased initially, but reached an optimum that occurred before solar noon owing to the flattening of the photosynthetic light response curve and stomatal closure with increasing VPD. The time of maximum absorbed radiation values happened around the same time (solar noon) for all canopies, but the time of maximal A varied among the different leaf angle cases. For instance, at high LAI, erectophile and spherical canopies had maximum A values between 10:00 and 11:00 h and uniform and planophile between 9:00 and 10:00 h. This is likely to be because, at high LAI, canopies with leaves tending towards horizontal become saturated with light earlier in comparison to canopies with leaves tending towards vertical.

The instantaneous whole-canopy fluxes of E increased as LAI increased and reached maximum values in the afternoon owing to the increase in VPD driven by ambient weather conditions. This corresponded to a similar diurnal peak in leaf temperature, T_s . These patterns suggest that E_c was more closely coupled with the ambient air than incident radiation for the chosen weather conditions.

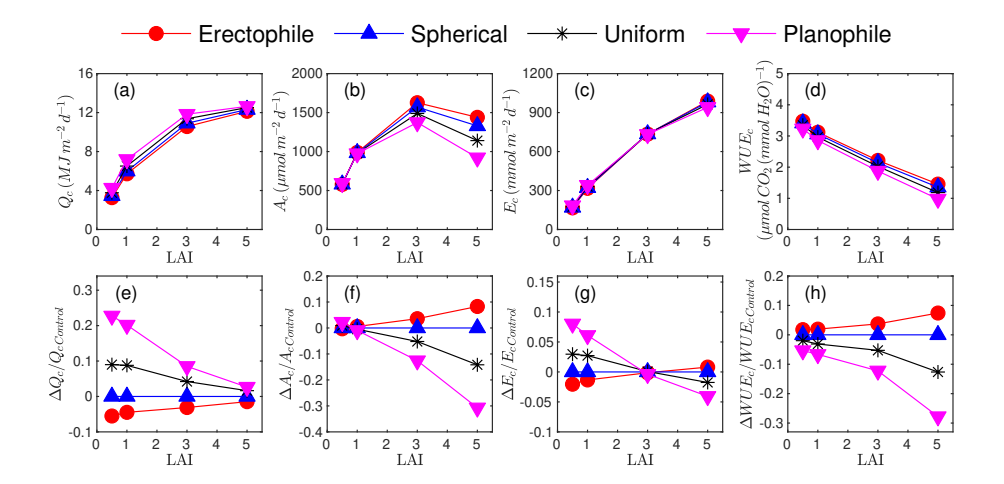


Figure 4: Daily absorbed radiation (Q_c) , photosynthesis (A_c) , transpiration (E_c) , and canopy water use efficiency (WUE_c) for the homogeneous canopy cases with four different leaf inclination distributions (isotropic azimuth distribution): erectophile, spherical, uniform, and planophile and with four different leaf area index (LAI) values: 0.5, 1, 3 and 5. (a-d) Daily integrated fluxes, (e-h) normalized difference (Δ) relative to the spherical leaf angle distribution (control case).

Overall, the effect of the leaf angle on E was small throughout the day, which is consistent with weak radiative coupling. In contrast, the effect of leaf angle on instantaneous whole-canopy fluxes of WUE varied slightly during the day and increased between 8:00 and 11:00 h at high LAI. The WUE values tended to be largest in the morning for all cases and were greater at low LAI. The lower WUE in the afternoon could be explained by the fact that E can increase continually for much of the day owing to a more linear response to light and increasing ambient VPD, whereas A begins to decline earlier in the day.

When LAI is low (Fig. 6a-e), variation in the leaf angle distribution causes a shift in the vertical profile relative to the spherical distribution that is fairly uniform with height and varies roughly according to the respective value of G (see Fig. 3a at 12:00 h). Absorbed radiation, net photosynthesis, transpiration, WUE and leaf temperature at a given height all tend to increase with respect to the spherical case according to G at low LAI.

When LAI < 1, there is minimal overlap between leaves, and thus the average absorbed radiation flux is nearly proportional to G. When LAI is much greater than 1 (Fig. 6f-j), similar behaviour is observed at 12:00 h in the upper canopy as for low LAI, but absorbed radiation tends to decrease relative to the spherical case with depth into the canopy when G > 0.5 and increase with depth when G < 0.5. There is some critical depth within the canopy at which the trend in absorbed radiation with G reverses. This crossover height is different for each of the variables considered in Fig. 6. It occurs at $\sim 40\%$ of the canopy height for G, 90% of the canopy height for G, 1 There was no crossover point for WUE, whereby

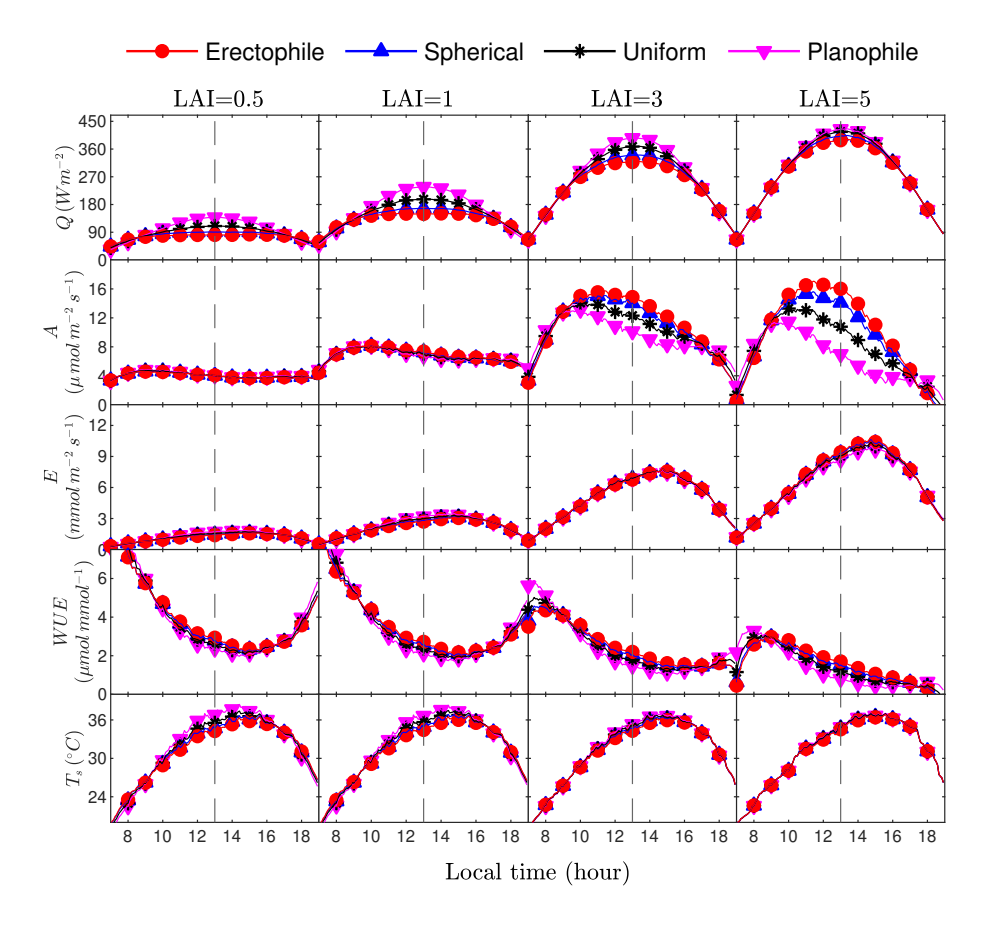


Figure 5: Instantaneous whole-canopy fluxes of absorbed radiation (Q), photosynthesis (A), transpiration (E), water use efficiency (WUE), and canopy temperature (T_s) for the homogeneous canopy cases with four different leaf angle distributions (isotropic azimuth distribution): erectophile, spherical, uniform, and planophile and with four different leaf area index (LAI) values: 0.5, 1, 3 and 5. The dashed vertical line indicates the time at solar noon.

WUE was always less than that of the spherical case when G > 0.5 and greater than the spherical case when G < 0.5. Variation in the crossover height relative to that of Q appears to be driven by the non-linearity of the response of the variables to light.

3.1.2. Effect of azimuthal anisotropy in a homogeneous canopy

Adding azimuthal anisotropy to the leaf angle distribution increased daily absorbed radiation by $\lesssim 11\%$ when leaf azimuths biased toward E-W and reduced daily absorbed radiation by $\lesssim 13\%$ when biased toward the N-S (Fig. 7). These differences agreed roughly with corresponding differences in G_{avg} (Fig. 3d). This suggested that more light could be captured over a day by E-W leaves than N-S leaves by maximizing light interception in the early and late day, rather

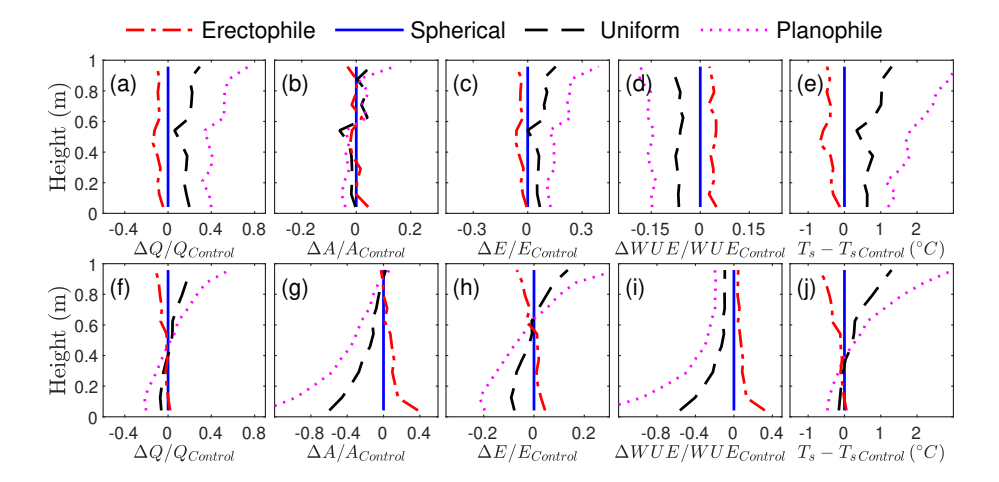


Figure 6: Vertical profiles of normalized difference (Δ) relative to the control (spherical leaf angle distribution) of absorbed radiation (Q), photosynthesis (A), transpiration (E), wateruse efficiency (WUE), and canopy temperature (T_s) for the homogeneous canopy cases with four different leaf angle distributions: erectophile, spherical, uniform, and planophile and two different leaf area index (LAI) values: 0.5 (a-e) and 3 (f-j) at 12:00 hours. The canopy height is 1 m.

than only mid-day. The effect of azimuthal anisotropy on absorbed radiation diminished as LAI increased, as was also observed for leaf inclination anisotropy (Fig. 4), which is because denser canopies are able to absorb nearly all incoming light regardless of the value of G. Light interception also became less sensitive to azimuthal anisotropy as G_{avg} increased. This is because for a vertical leaf, changing azimuth has the possibility to move the leaf between full sun and full shade, whereas light interception of a horizontal leaf does not change with azimuth.

At high LAI, net photosynthesis was reduced relative to the azimuthally isotropic canopy when leaf azimuths were biased towards E–W and increased when azimuths were biased towards N–S. For the erectophile, spherical and uniform canopies, this trend reversed below an LAI of one or two. Daily-averaged G increased for leaf azimuths biased towards E–W and decreased for leaf azimuths biased towards N–S, with planophile G_{avg} being least affected by azimuthal anisotropy(Fig. 3d). It is expected that N-S biased azimuths, for example, should have a similar effect as increasing LAI or G in the azimuthally isotropic cases (Fig. 4). This is in fact the trend that was observed: N–S-biased leaf azimuths increased photosynthesis at high LAI by allowing additional penetration of light into the canopy, whereas it decreased photosynthesis at low LAI owing to light lost to the ground. The effect was similar for transpiration and WUE. N–S-biased azimuths increased transpiration at high LAI and decreased transpiration at low LAI, with the planophile canopies having the least sensitivity to leaf azimuthal anisotropy. The WUE was increased with N–S-biased leaf azimuths, which was amplified with increasing LAI.

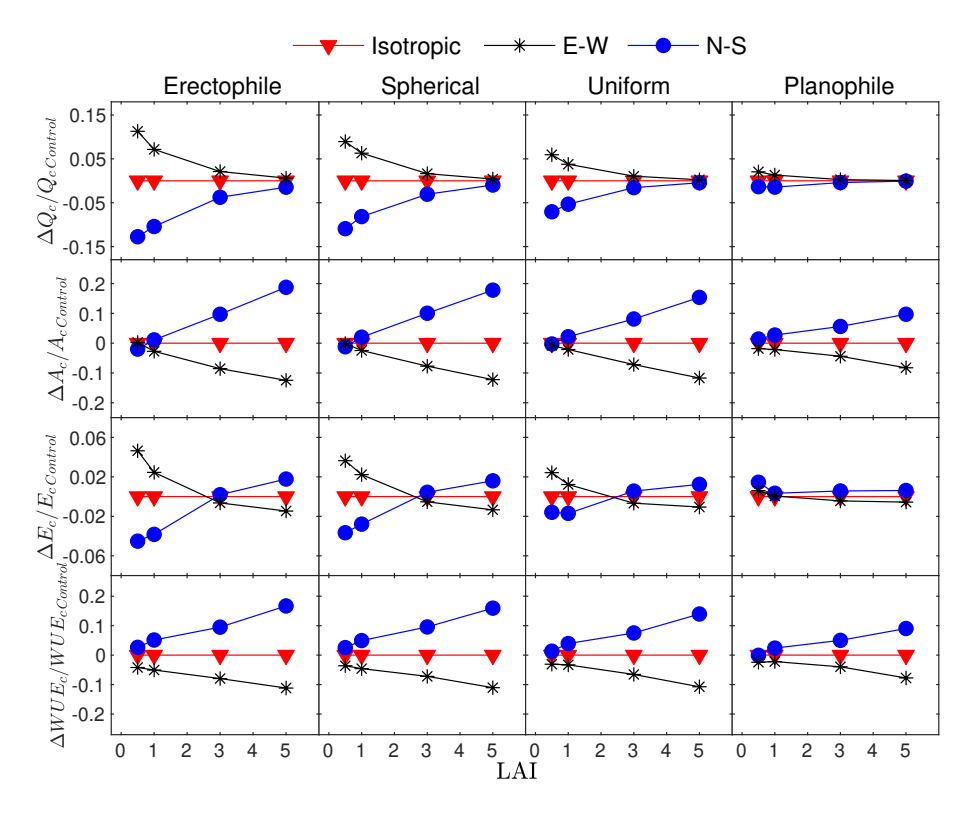


Figure 7: Normalized difference (Δ) relative to the control (isotropic leaf azimuth) in daily integrated absorbed radiation (Q_c), photosynthesis (A_c), transpiration (E_c), and canopy water use efficiency (WUE_c) owing to anisotropic leaf azimuth for the homogeneous canopy cases with four different leaf inclination distributions: erectophile, spherical, uniform and planophile and with four different leaf area index (LAI) values: 0.5, 1, 3 and 5.

3.2. Case 2: effect of heterogeneity

The addition of canopy heterogeneity at constant leaf area density generally tended to decrease daily absorbed radiation, net photosynthesis and transpiration (Fig. 8). This is expected because there is less leaf area overall when leaf area per ground area is removed to increase heterogeneity. Increasing heterogeneity also increased $WUE_c \lesssim 130\%$ relative to the homogeneous canopy, while decreasing daily net photosynthesis by $\sim 60\%$ for the same case (Fig. 9). Although increasing plant spacing reduced both photosynthesis and transpiration owing to the associated reduction in overall leaf area per ground area, it tended to reduce transpiration more than photosynthesis. Most of the WUE gains occurred up to a plant spacing of ~ 2 m, beyond which there was little change in WUE.

Interestingly, there were cases in which removing canopy leaf area could increase net photosynthesis, A_c . This occurred for cases with leaves biased towards horizontal (uniform and planophile) when the canopy was transitioned

from homogeneous to spherical crowns with the smallest row spacing. It is expected that this is attributable to a similar mechanism that created a decline in A_c in the homogeneous canopies when LAI was increased above three. Decreasing leaf area can result in a more efficient vertical light distribution when overall light absorption is high.

As heterogeneity increased, hourly whole-canopy fluxes of Q reduced per ground area, hence A and E decreased. However, WUE increased in the heterogeneous canopy compared to the homogeneous canopy by $\lesssim 270\%$ in the afternoon (Fig. 9). The largest increases in WUE as G was varied occurred in the horizontally-biased leaf angle cases during the afternoon when VPD was high. The effect of leaf inclination distribution on WUE was greater in the planophile leaf angle distribution case compared with the erectophile case because leaves in the planophile distribution are much more biased towards horizontal leaves than the erectophile distribution is biased towards vertical leaves (Fig. 1b).

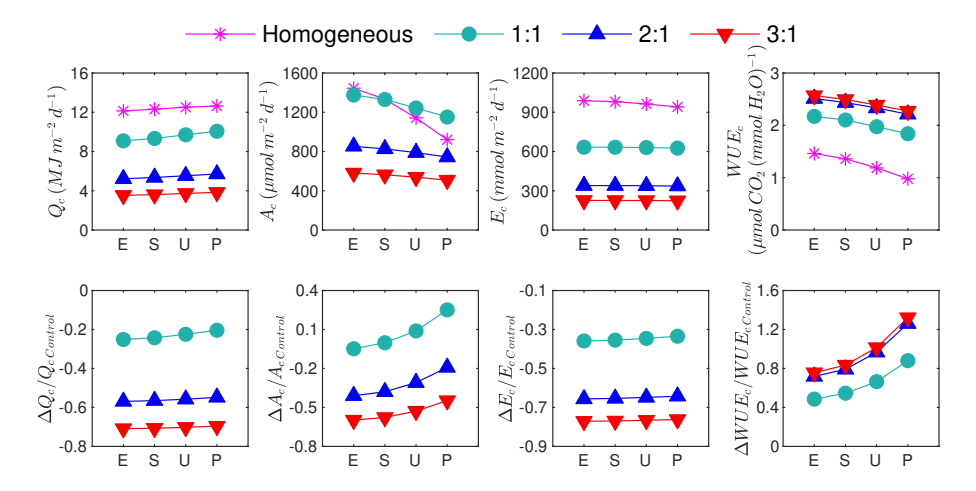


Figure 8: Cumulative and normalized difference (Δ) relative to the control (homogeneous canopy case) of daily integrated absorbed radiation (Q_c) , photosynthesis (A_c) , transpiration (E_c) , and canopy water use efficiency (WUE_c) between a range of hypothetical heterogeneous canopies and their corresponding homogeneous canopy case. For the heterogeneous canopy cases, each line corresponds to cases with different ratio between row spacing and canopy height (1 m). All canopies had the same leaf area density $(5 \text{ m}^2 \text{ m}^{-3})$ and included homogeneous and heterogeneous canopies with isotropic leaf inclination angle (S=spherical), and anisotropic leaf inclination (E=erectophile, U=uniform, P=planophile). The heterogeneous canopy was oriented in N-S rows and in three different row spacings: 1 m (canopy-level LAI= 2.6), 2 m (canopy-level LAI= 1.3) and 3 m (canopy-level LAI= 0.9).

3.2.1. Effect of physiological parameter variation

Variation in V_{cmax25} (and by extension J_{max25} and R_{d25}) over nearly an order of magnitude had a significant effect on the impact of leaf angle on WUE_c (Fig. 10a-c). Increasing photosynthetic capacity via V_{cmax25} increases the magnitude of WUE_c , and the normalized values of WUE_c shown in Fig. 10a-c suggest

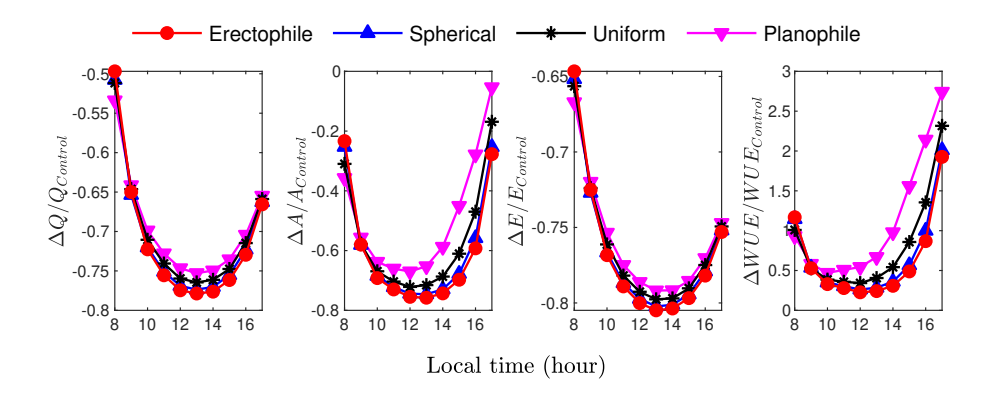


Figure 9: Difference in instantaneous whole-canopy fluxes of absorbed radiation (Q), photosynthesis (A), transpiration (E), and water use efficiency (WUE) between canopies with 3 m row spacing (canopy-level LAI= 0.9) and their corresponding homogeneous canopy (control) with the same leaf area density $(5 \text{ m}^2 \text{ m}^{-3})$. The canopies were oriented in N-S rows and included heterogeneous canopies with isotropic (spherical) and anisotropic leaf inclination angles (erectophile, uniform, and planophile).

that this increase has a relatively small impact on WUE at low V_{cmax25} across canopy cases and becomes increasingly significant at high V_{cmax25} .

Variation in the initial slope of the photosynthetic light response curve by changing the value of α did have a notable impact on the relationship between leaf angle and WUE_c (Fig. 10d-f). Varying α shifted the LAI value at which WUE_c increased or decreased relative to the spherical canopy when G_{avg} was varied. At low LAI, WUE_c increased with respect to the spherical canopy as G_{avg} increased. At some critical LAI value that decreased as α increased, this trend reversed. Increasing α causes photosynthesis to saturate at lower light levels. Thus, it is expected that decreasing α should cause an increase in WUE_c relative to the spherical canopy for leaf angle distributions biasing towards horizontal because it increases photosynthesis for the relatively large amount of low-light leaves in the lower canopy shaded by overlying leaf layers.

Increasing the maximum transpiration rate, E_m , decreased sensitivity of WUE_c to leaf angle. Increasing E_m tends to increase the contribution of E_c to WUE_c . As was shown above, E_c is much less sensitive to the leaf angle distribution than A_c . Thus, it follows that increasing the contribution of E_c to WUE_c should decrease sensitivity of WUE_c to the leaf angle distribution.

4. Discussion

4.1. Optima in WUE and photosynthesis with varying canopy architecture

Optimizing canopy structure to improve WUE has been proposed as an approach for producing more efficient crops under the changing climate (Drewry et al., 2014; Srinivasan et al., 2017; Hatfield and Dold, 2019). The results suggested that canopy structure could have a significant influence on both instantaneous and daily-integrated WUE. Within the range of homogeneous canopy

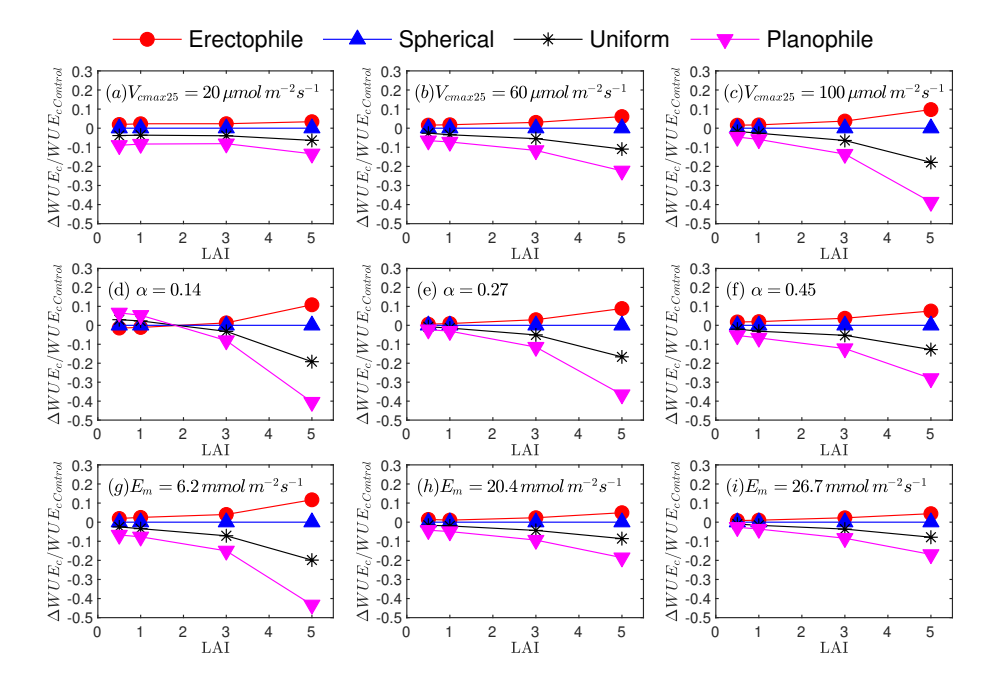


Figure 10: Analyses of physiological parameters on WUE where V_{cmax25} was varied from 78.5 (reference) to 20, 60, and 100 μ mol m⁻² s⁻¹, R_{d25} was varied according to Eq. 20 from 2.1 (reference) to 0.5, 1,6 and 2.7 μ mol m⁻² s⁻¹, and J_{max25} was varied according to Eq. 19 from 133 (reference) to 39.5, 105 and 165 μ mol m⁻² s⁻¹, respectively (a-c). The parameter values of α were reduced from 0.45 (reference) to 0.27 and 0.14 (d-f) and E_m was varied from 20.5 (reference) 6.2, 12.3, and 26.7 mmol m⁻² s⁻¹ (g-i), respectively. The data plotted is for homogeneous canopies with leaf area index (LAI) of 0.5, 1, 3 and 5.

cases considered, WUE varied among the cases by >100% at a given hour and by nearly 35% on a daily basis (mainly owing to LAI). High LAI tended to amplify the effect of leaf angle on WUE. Introducing canopy heterogeneity could create further increases in WUE.

Despite the pronounced effect of canopy structure on WUE, there did not appear to be a distinct optimum in WUE as LAI, leaf angle distribution or heterogeneity was varied. WUE decreased monotonically as LAI, G_{avg} , or homogeneity were increased. Intuitively, it seems as though an instantaneous optimum in WUE_c could exist. At the leaf level, there is an optimum in WUE with respect to light at the so-called "breakpoint" of the photosynthetic light response curve (Kao and Forseth, 1992). Thus, a leaf angle distribution that minimizes self-shading and orients leaves such that radiative fluxes are near the breakpoint should be optimal. However, it might be that the limited flexibility of the four leaf angle distributions with isotropic azimuths did not find the optimum. It is also possible that an instantaneous optimum might exist, but that it cannot be maintained over an entire day without leaf solar tracking. This was estimated in slash pine and $Schima\ superba$, in which WUE_c was positively

correlated with light, leaf temperature and VPD; however, after the breakpoint, WUE_c decreased with light, leaf temperature and VPD (Zhuang et al., 2023)

Despite the lack of an observed WUE optimum, there was a distinct optimum in daily net photosynthesis, A_c , with varying LAI, as has been reported in previous experimental studies (Digrado et al., 2020), which was attributable to the trade-off between productivity and respiratory costs via increasing leaf area. This optimum in A_c did not translate into an optimum in WUE because the denominator of WUE, E_c , continues to increase as LAI increases owing to the fact that sunlit and shaded leaf area contribute positively to E_c whereas shaded leaf area tends to contribute negatively to A_c .

In our study, it was assumed that photosynthetic properties were uniform throughout the canopy. However, in real canopies, V_{cmax} would be smaller where light is lower, and respiration would tend to decline proportionately (Buckley et al., 2013). This could potentially result in less of a carbon 'cost' owing to shaded leaves and could affect the optimum in A_c observed at moderate LAI (see Fig. 4). For instance, in corn at high density, removal of two leaves above the ear resulted in a 14 % increase in photosynthesis (Liu et al., 2015). Despite this over simplification based on uniform photosynthetic properties, our results for all the different leaf orientation cases agree with field observations in cowpea (Digrado et al., 2020) and soybean (Srinivasan et al., 2017), which observed an optimum in A_c at a similar LAI of around three.

Introducing canopy-scale heterogeneity monotonically increased WUE for an individual plant at the expense of whole canopy productivity, and thus there was no clear optimum in WUE with varying plant density. However, in some cases there was an optimum in A_c . For the uniform and planophile leaf angle distributions, the smallest plant spacing (1:1) increased A_c relative to the homogeneous canopy, but then A_c declined for a 2:1 plant spacing (Fig. 8). This optimum is probably attributable to the same mechanism causing the optimum in A_c when LAI is varied in the homogeneous canopies. A small amount of heterogeneity allows for increased light penetration and increases the fraction of sunlit leaf area, and thus increases net photosynthesis. If this increase in net photosynthesis is larger than the overall reduction in total leaf area resulting from the heterogeneity, net photosynthesis can increase.

4.2. Leaf inclination angle anisotropy

Anisotropy in the leaf inclination angle distribution has increasingly become a trait of interest in terms of its influence on canopy gas and energy exchange processes (e.g, Van Zanten et al., 2010; Mantilla-Perez and Salas Fernandez, 2017; Pisek et al., 2022). For instance, land surface models can represent temperate and boreal broadleaf forests as canopies that tend to have leaves towards the horizontal direction rather than assuming a spherical leaf inclination angle distribution (Bonan et al., 2011). This study provided additional insight into the effect of leaf inclination angle anisotropy on canopy transpiration and WUE. The largest impacts of leaf inclination angle distribution on light interception occurred when LAI was small and on photosynthesis and WUE when LAI was high. When LAI is small (e.g., young canopy), the largest gains in light

interception and photosynthesis are attained by increasing LAI, although this comes at an increasingly expensive water cost. As the canopy develops, there are diminishing returns on increasing LAI, and leaf angle becomes increasingly important for productivity. A transition to more vertical leaf angle distribution at this point might be beneficial not only in terms of increasing photosynthesis, but also WUE. Daily photosynthesis varied by 39% and daily WUE by 36% across all leaf angle distributions considered when LAI = 5.

It is also noteworthy that daily transpiration varied between all cases considered by < 10% relative to the corresponding spherical leaf angle distribution case, whereas daily photosynthesis and WUE could vary by > 30%. This is probably attributable to the fact that the difference in relative transpiration rate between a leaf perpendicular and parallel to the sun is much smaller than for relative photosynthesis.

4.3. Leaf azimuthal angle anisotropy

Anisotropy in leaf azimuth is rarely considered in models or field experiments, although it can have a similar impact as anisotropy in leaf inclination. Previous work has illustrated that leaf azimuthal anisotropy can amplify the effects of canopy heterogeneity (Ponce de León and Bailey, 2019). For instance, in row-oriented canopies, the effective path length of the sun's rays through vegetation can change dramatically with changes in sun azimuth, which is important in agricultural canopy design applications, such as to reduce the effect of elevated temperatures in vineyards (Ponce de León and Bailey, 2022). The present work also explored the effect of leaf azimuth on canopy biophysical processes. In canopies with high LAI, simulation results suggested that biasing leaf normals towards the N–S directions in an erectophile canopy increased A_c and WUE_c by $\sim 30\%$ relative to E-W biased leaves. This finding is consistent with field experiments that reported a $\sim 25\%$ and $\sim 22\%$ increase in A_c and WUE_c , respectively, for vertical leaves biased toward N-S compared with E-W (Smith and Ullberg, 1989).

For canopy-level models applied to sparse natural canopies or row-oriented crops, consideration of leaf azimuthal anisotropy within radiation attenuation coefficients might have an important effect on model predictions, particularly in canopies with leaf inclination tending towards vertical. Although leaf (inclination) angle has become a trait of increasing interest for ecosystem ecology, plant physiology and remote sensing (e.g., Pisek et al., 2022; Yang et al., 2023), measurement and consideration of leaf azimuth might warrant attention in addition to the more common practice of measuring leaf inclination angle only (e.g., Daviet et al., 2022; Serouart et al., 2023). Fortunately, techniques now exist for high-throughput measurement of leaf inclination and azimuth from Li-DAR scanning data (e.g., Bailey and Mahaffee, 2017) and from accelerometers integrated within leaf-level measurement devices, such as the LICOR LI-600 porometer (LICOR Biosciences, Lincoln, NE, USA).

4.4. Canopy heterogeneity

The results suggested that canopy heterogeneity can have a significant effect on biophysical processes related to WUE, yet the majority of plant system models are based on assumptions of canopy homogeneity or include heterogeneity through empirically tunable parameters (e.g, Sellers et al., 1992; Sykes et al., 2001; Lawrence et al., 2019). The least heterogeneous discontinuous canopy case considered was still relatively homogeneous, with a crown ground cover fraction of 78%. Nevertheless, this amount of heterogeneity decreased E_c by $\sim 36\%$, and increased WUE_c by $\sim 88\%$. The effect of adding this small amount of heterogeneity was minimal for A_c due to offsetting effects of the increase in light distribution efficiency and decrease in total leaf area. The impact of heterogeneity on WUE_c for plant spacing larger than 2:1 was minimal, because at this point the crowns were almost fully isolated, and WUE is not impacted by reduction in leaf area on a ground area basis because it is a ratio.

4.5. Linkage between leaf area, leaf angle distribution, and heterogeneity

By and large, the effect of increasing LAI, increasing G_{avg} , and increasing homogeneity (at constant leaf area density) had a similar effect on daily-integrated canopy fluxes. Variation of these parameters in this way generally leads to increased light interception owing to the resulting increase in projected leaf area. This tends to increase canopy photosynthesis at low LAI, primarily because of the increase in total light available to the canopy, and decreases canopy photosynthesis at high LAI owing to inefficient utilization of light throughout the canopy depth. This additional light increases canopy transpiration owing to additional available energy and transpiring surface area in the case of increasing LAI. Increased light interception tended to cause a monotonic decrease in WUE_c .

4.6. Limitations and future work

A limitation of the proposed study is the lack of direct experimental validation. However, it is extremely difficult to vary interacting parameters systematically within field experiments. Natural variation in canopy structure over time or space will inherently be confounded by associated changes in environmental or physiological variables, not to mention that reliably measuring the variables associated with this canopy structure is difficult. Measurement of canopy-scale WUE is additionally difficult, owing to non-vegetative and non-local contributions to water vapour and CO₂ fluxes. In this study, the simulated data were generated by a 3D leaf-resolving model, in which the exact inputs were known. Each of the model sub-components is physically based and has been validated independently. Virtual experiments establish a theoretical basis for guiding field experiments and future reduced-order modelling studies, which could be expanded to short- and long-term leaf responses of WUE to environmental conditions. For instance, studying the leaf response to elevated temperatures or droughts could provide valuable information for breeding climate-resilient cultivars.

In real canopies, plant architectural and physiological traits vary with height and laterally within the canopy owing to structural heterogeneity (Niinemets, 1998, 2010; Buckley et al., 2013; Raabe et al., 2015). In order to make the present study tractable, leaf area density, leaf angle distribution, radiative properties and physiological parameters were assumed constant in space. There is no doubt that including such variation would impact results, but the underlying principles are expected to be the same. The models used in this work are fully capable of representing arbitrarily complex spatial distributions of these traits, which could be used as a tool for future exploration of how these traits are distributed in real canopies and how this impacts canopy-scale fluxes.

Only a single representative weather scenario without diffuse solar radiation, and a single location, was considered, although it is known that weather and geographical conditions can have a significant impact on WUE (Tan et al., 2015; Dekker et al., 2016). Because of the large number of variables already considered in this work, it was not possible also to explore in depth the effects of different weather scenarios and geographical conditions. Although it is clear that variation in specified weather inputs would have a significant effect on the magnitude of fluxes related to WUE, it is expected that overall trends should hold for a wide range of conditions. Extreme conditions that cause near stomatal closure, excessively high respiration rates or very small photosynthetic rates owing to cold temperatures, for example, could cause transitional behaviour. If the canopy location was chosen to be at a different latitude, this would affect the day length and minimum solar zenith angle, which could have an effect on daily integrated fluxes. For example, at higher latitudes the daily light interception is expected to increase in the erectophile canopies and decrease in the planophile canopies. It is expected that addition of diffuse radiation should decrease the impact of the leaf angle distribution, because leaf angle has no impact when incident radiation is isotropic. Further work is needed to explore whether and when weather and geographical conditions can cause transitional behaviour in the interactions between WUE and canopy architecture

5. Conclusion

The results showed that variations in leaf area and leaf angle could have a substantial effect on WUE and that the effect of leaf angle increases as canopy density increases or heterogeneity decreases. There was no observed optimum in WUE as LAI, the leaf angle distribution or heterogeneity was varied. There was, however, an optimum in daily canopy photosynthesis with increasing light interception owing to the trade-off between the increase in photosynthesis with increasing available light and the decrease in photosynthesis owing to respiratory costs of shaded leaf area. It can thus be concluded that leaf angle and density traits might be viable targets for increasing crop productivity through breeding or through management practices, such as pruning and thinning. Results suggested that in dense canopies, reduction in vegetation density through thinning or biasing leaf angles towards the vertical could simultaneously increase photosynthesis and WUE. Furthermore, the potentially high impact of these

architectural traits on WUE motivates their explicit representation within land surface models, and their accurate specification as model inputs. More work is needed to investigate thoroughly leaf solar tracking or other traits that could permit optima in WUE with varying architecture.

Acknowledgements

This work was financially support by the USDA National Institute of Food and Agriculture, Hatch project number 1013396, and U.S. National Science Foundation grant IOS 2047628.

References

- Bailey, B.N., 2018. A reverse ray-tracing method for modelling the net radiative flux in leaf-resolving plant canopy simulations. Ecological Modelling 368, 233–245.
- Bailey, B.N., 2019. Helios: a scalable 3D plant and environmental biophysical modeling framework. Frontiers in Plant Science 10, 1185.
- Bailey, B.N., Kent, E.R., 2021. On the resolution requirements for accurately representing interactions between plant canopy structure and function in three-dimensional leaf-resolving models. in silico Plants 3, diab023.
- Bailey, B.N., Mahaffee, W.F., 2017. Rapid measurement of the three-dimensional distribution of leaf orientation and the leaf angle probability density function using terrestrial lidar scanning. Remote Sensing of Environment 194, 63–76.
- Bernacchi, C., Pimentel, C., Long, S.P., 2003. *In vivo* temperature response functions of parameters required to model RuBP-limited photosynthesis. Plant, Cell & Environment 26, 1419–1430.
- Bernacchi, C., Singsaas, E., Pimentel, C., Portis Jr, A., Long, S., 2001. Improved temperature response functions for models of Rubisco-limited photosynthesis. Plant, Cell & Environment 24, 253–259.
- Bonan, G.B., Lawrence, P.J., Oleson, K.W., Levis, S., Jung, M., Reichstein, M., Lawrence, D.M., Swenson, S.C., 2011. Improving canopy processes in the Community Land Model version 4 (CLM4) using global flux fields empirically inferred from FLUXNET data. Journal of Geophysical Research: Biogeosciences 116, G02014.
- Buckley, T.N., Cescatti, A., Farquhar, G.D., 2013. What does optimization theory actually predict about crown profiles of photosynthetic capacity when models incorporate greater realism? Plant, Cell & Environment 36, 1547–1563.

- Buckley, T.N., Turnbull, T.L., Adams, M.A., 2012. Simple models for stomatal conductance derived from a process model: cross-validation against sap flux data. Plant, Cell & Environment 35, 1647–1662.
- Campbell, G.S., Norman, J.M., 1998. Radiation fluxes in natural environments, in: An introduction to environmental biophysics. Springer, pp. 167–184.
- Chelle, M., Andrieu, B., 1998. The nested radiosity model for the distribution of light within plant canopies. Ecological Modelling 111, 75–91.
- Condon, A.G., Richards, R., Rebetzke, G., Farquhar, G., 2004. Breeding for high water-use efficiency. Journal of experimental botany 55, 2447–2460.
- Daviet, B., Fernandez, R., Cabrera-Bosquet, L., Pradal, C., Fournier, C., 2022. PhenoTrack3D: an automatic high-throughput phenotyping pipeline to track maize organs over time. Plant Methods 18, 130.
- De Pury, D., Farquhar, G., 1997. Simple scaling of photosynthesis from leaves to canopies without the errors of big-leaf models. Plant, Cell & Environment 20, 537–557.
- de Wit, C.T., 1965. Photosynthesis of Leaf Canopies. Agricultural Research Report 663. Wageningen. pp. 57.
- Dekker, S.C., Groenendijk, M., Booth, B.B., Huntingford, C., Cox, P.M., 2016. Spatial and temporal variations in plant water-use efficiency inferred from tree-ring, eddy covariance and atmospheric observations. Earth System Dynamics 7, 525–533.
- Digrado, A., Mitchell, N.G., Montes, C.M., Dirvanskyte, P., Ainsworth, E.A., 2020. Assessing diversity in canopy architecture, photosynthesis, and wateruse efficiency in a cowpea magic population. Food and Energy Security 9, e236.
- Drewry, D.T., Kumar, P., Long, S.P., 2014. Simultaneous improvement in productivity, water use, and albedo through crop structural modification. Global change biology 20, 1955–1967.
- Ehleringer, J., Werk, K., 1986. Modifications of solar-radiation absorption patterns and implications for carbon gain at the leaf level, in: On the economy of plant form and function: proceedings of the Sixth Maria Moors Cabot Symposium, Evolutionary Constraints on Primary Productivity, Adaptive Patterns of Energy Capture in Plants, Harvard Forest, August 1983, Cambridge University Press. pp. 57–82.
- Ezcurra, E., Montana, C., Arizaga, S., 1991. Architecture, light interception, and distribution of larrea species in the monte desert, argentina. Ecology 72, 23–34.

- Falster, D.S., Westoby, M., 2003. Leaf size and angle vary widely across species: what consequences for light interception? New Phytologist 158, 509–525.
- Farquhar, G.D., von Caemmerer, S., Berry, J.A., 1980. A biochemical model of photosynthetic CO₂ assimilation in leaves of C3 species. Planta 149, 78–90.
- Foley, J.A., Prentice, I.C., Ramankutty, N., Levis, S., Pollard, D., Sitch, S., Haxeltine, A., 1996. An integrated biosphere model of land surface processes, terrestrial carbon balance, and vegetation dynamics. Global Biogeochemical Cycles 10, 603–628.
- Forrester, D.I., Collopy, J.J., Beadle, C.L., Warren, C.R., Baker, T.G., 2012. Effect of thinning, pruning and nitrogen fertiliser application on transpiration, photosynthesis and water-use efficiency in a young *Eucalyptus nitens* plantation. Forest Ecology and Management 266, 286–300.
- Forseth, I., Ehleringer, J., 1983. Ecophysiology of two solar tracking desert winter annuals. Oecologia 58, 10–18.
- Goel, N.S., Strebel, D.E., 1984. Simple beta distribution representation of leaf orientation in vegetation canopies 1. Agronomy Journal 76, 800–802.
- Gueymard, C.A., 2008. REST2: High-performance solar radiation model for cloudless-sky irradiance, illuminance, and photosynthetically active radiation–validation with a benchmark dataset. Solar Energy 82, 272–285.
- Hatfield, J.L., Dold, C., 2019. Water-use efficiency: advances and challenges in a changing climate. Frontiers in plant science 10, 103.
- Henke, M., Buck-Sorlin, G.H., 2017. Using a full spectral raytracer for calculating light microclimate in functional-structural plant modelling. Computing and Informatics 36, 1492–1522.
- Humphries, S., Long, S., 1995. WIMOVAC: a software package for modelling the dynamics of plant leaf and canopy photosynthesis. Bioinformatics 11, 361–371.
- James, S.A., Bell, D.T., 2000. Leaf orientation, light interception and stomatal conductance of *Eucalyptus globulus* ssp. *globulus* leaves. Tree Physiology 20, 815–823.
- Jin, S., Wang, Y., Shi, L., Guo, X., Zhang, J., 2018. Effects of pruning and mulching measures on annual soil moisture, yield, and water use efficiency in jujube (*Ziziphus jujube Mill.*) plantations. Global ecology and conservation 15, e00406.
- Jones, C., Dyke, P., Williams, J., Kiniry, J., Benson, V., Griggs, R., 1991. EPIC: an operational model for evaluation of agricultural sustainability. Agricultural Systems 37, 341–350.

- Jones, J.W., Hoogenboom, G., Porter, C.H., Boote, K.J., Batchelor, W.D., Hunt, L., Wilkens, P.W., Singh, U., Gijsman, A.J., Ritchie, J.T., 2003. The DSSAT cropping system model. European Journal of Agronomy 18, 235–265.
- Kao, W.Y., Forseth, I., 1992. Dirunal leaf movement, chlorophyll fluorescence and carbon assimilation in soybean grown under different nitrogen and water availabilities. Plant, Cell & Environment 15, 703–710.
- Kao, W.Y., Tsai, T.T., Chen, W.H., 1998. Response of photosynthetic gas exchange and chlorophyll a fluorescence of *Miscanthus floridulus* (Labill) Warb. to temperature and irradiance. Journal of Plant Physiology 152, 407–412.
- Knauer, J., Zaehle, S., Medlyn, B.E., Reichstein, M., Williams, C.A., Migliavacca, M., De Kauwe, M.G., Werner, C., Keitel, C., Kolari, P., et al., 2018. Towards physiologically meaningful water-use efficiency estimates from eddy covariance data. Global Change Biology 24, 694–710.
- Kustas, W.P., Norman, J.M., 1999. Evaluation of soil and vegetation heat flux predictions using a simple two-source model with radiometric temperatures for partial canopy cover. Agricultural and Forest Meteorology 94, 13–29.
- Lawrence, D.M., Fisher, R.A., Koven, C.D., Oleson, K.W., Swenson, S.C., Bonan, G., Collier, N., Ghimire, B., van Kampenhout, L., Kennedy, D., et al., 2019. The Community Land Model version 5: Description of new features, benchmarking, and impact of forcing uncertainty. Journal of Advances in Modeling Earth Systems 11, 4245–4287.
- Le Roux, X., Bariac, T., Sinoquet, H., Genty, B., Piel, C., Mariotti, A., Girardin, C., Richard, P., 2001. Spatial distribution of leaf water-use efficiency and carbon isotope discrimination within an isolated tree crown. Plant, Cell & Environment 24, 1021–1032.
- Ponce de León, M.A., Bailey, B.N., 2019. Evaluating the use of Beer's law for estimating light interception in canopy architectures with varying heterogeneity and anisotropy. Ecological Modelling 406, 133–143.
- Ponce de León, M.A., Bailey, B.N., 2021. A 3D model for simulating spatial and temporal fluctuations in grape berry temperature. Agricultural and Forest Meteorology 306, 108431.
- Ponce de León, M.A., Bailey, B.N., 2022. Fruit zone shading to control grape berry temperature: A modeling study. American Journal of Enology and Viticulture 73, 183–197.
- Liu, T., Gu, L., Dong, S., Zhang, J., Liu, P., Zhao, B., 2015. Optimum leaf removal increases canopy apparent photosynthesis, 13c-photosynthate distribution and grain yield of maize crops grown at high density. Field Crops Research 170, 32–39.

- Lloyd, J., Grace, J., Miranda, A.C., Meir, P., Wong, S., Miranda, H.S., Wright, I., Gash, J., McIntyre, J., 1995. A simple calibrated model of Amazon rainforest productivity based on leaf biochemical properties. Plant, Cell & Environment 18, 1129–1145.
- Long, S., Farage, P., Garcia, R., 1996. Measurement of leaf and canopy photosynthetic $\rm CO_2$ exchange in the field. Journal of Experimental Botany 47, 1629-1642.
- Long, S.P., Zhu, X.G., Naidu, S.L., Ort, D.R., 2006. Can improvement in photosynthesis increase crop yields? Plant, Cell & Environment 29, 315–330.
- López, A., Molina-Aiz, F., Valera, D., Peña, A., 2012. Determining the emissivity of the leaves of nine horticultural crops by means of infrared thermography. Scientia Horticulturae 137, 49–58.
- Mahaffee, W.F., Margairaz, F., Ulmer, L.D., Bailey, B.N., Stoll, R., 2023. Catching spores: Linking epidemiology, pathogen biology, and physics to ground-based airborne inoculum monitoring. Plant Disease 107, 13–33.
- Mantilla-Perez, M.B., Salas Fernandez, M.G., 2017. Differential manipulation of leaf angle throughout the canopy: current status and prospects. Journal of Experimental Botany 68, 5699–5717.
- McPherson, R.A., 2007. A review of vegetation—atmosphere interactions and their influences on mesoscale phenomena. Progress in Physical Geography 31, 261–285.
- Nelson, J.A., Pérez-Priego, O., Zhou, S., Poyatos, R., Zhang, Y., Blanken, P.D., Gimeno, T.E., Wohlfahrt, G., Desai, A.R., Gioli, B., et al., 2020. Ecosystem transpiration and evaporation: Insights from three water flux partitioning methods across fluxnet sites. Global change biology 26, 6916–6930.
- Niinemets, Ü., 1998. Adjustment of foliage structure and function to a canopy light gradient in two co-existing deciduous trees. variability in leaf inclination angles in relation to petiole morphology. Trees 12, 446–451.
- Niinemets, Ü., 2010. A review of light interception in plant stands from leaf to canopy in different plant functional types and in species with varying shade tolerance. Ecological Research 25, 693–714.
- Ort, D.R., 2001. When there is too much light. Plant Physiology 125, 29–32.
- Pearcy, R.W., Yang, W., 1996. A three-dimensional crown architecture model for assessment of light capture and carbon gain by understory plants. Oecologia 108, 1–12.
- Pisek, J., Diaz-Pines, E., Matteucci, G., Noe, S., Rebmann, C., 2022. On the leaf inclination angle distribution as a plant trait for the most abundant broadleaf tree species in europe. Agricultural and Forest Meteorology 323, 109030.

- Prata, A., 1996. A new long-wave formula for estimating downward clearsky radiation at the surface. Quarterly Journal of the Royal Meteorological Society 122, 1127–1151.
- Raabe, K., Pisek, J., Sonnentag, O., Annuk, K., 2015. Variations of leaf inclination angle distribution with height over the growing season and light exposure for eight broadleaf tree species. Agricultural and Forest Meteorology 214, 2–11.
- Richards, R.A., Cavanagh, C.R., Riffkin, P., 2019. Selection for erect canopy architecture can increase yield and biomass of spring wheat. Field Crops Research 244, 107649.
- Ross, J., 1981. The radiation regime and architecture of plant stands. Dr. W. Junk Publishers, The Hague, The Netherlands. 424 pp.
- Schuepp, P., 1993. Tansley review No. 59. Leaf boundary layers. New Phytologist 125, 477–507.
- Sellers, P., Berry, J., Collatz, G., Field, C., Hall, F., 1992. Canopy reflectance, photosynthesis, and transpiration. III. A reanalysis using improved leaf models and a new canopy integration scheme. Remote sensing of environment 42, 187–216.
- Sellers, P., Randall, D., Collatz, G., Berry, J., Field, C., Dazlich, D., Zhang, C., Collelo, G., Bounoua, L., 1996. A revised land surface parameterization (SiB2) for atmospheric GCMs. Part I: Model formulation. Journal of Climate 9, 676–705.
- Serouart, M., Lopez-Lozano, R., Daubige, G., Baumont, M., Escale, B., De Solan, B., Baret, F., 2023. Analyzing changes in maize leaves orientation due to GxExM using an automatic method from RGB images. Plant Phenomics 5, 0046.
- Smith, M., Ullberg, D., 1989. Effect of leaf angle and orientation on photosynthesis and water relations in *Silphium terebinthinaceum*. American Journal of Botany 76, 1714–1719.
- Song, Q., Zhang, G., Zhu, X.G., 2013. Optimal crop canopy architecture to maximise canopy photosynthetic CO₂ uptake under elevated CO₂–a theoretical study using a mechanistic model of canopy photosynthesis. Functional Plant Biology 40, 108–124.
- Srinivasan, V., Kumar, P., Long, S.P., 2017. Decreasing, not increasing, leaf area will raise crop yields under global atmospheric change. Global Change Biology 23, 1626–1635.
- Sykes, M.T., Prentice, I.C., Smith, B., Cramer, W., Venevsky, S., 2001. An introduction to the European terrestrial ecosystem modelling activity. Global Ecology and Biogeography 10, 581–593.

- Tan, Z.H., Zhang, Y.P., Deng, X.B., Song, Q.H., Liu, W.J., Deng, Y., Tang, J.W., Liao, Z.Y., Zhao, J.F., Song, L., et al., 2015. Interannual and seasonal variability of water use efficiency in a tropical rainforest: Results from a 9 year eddy flux time series. Journal of Geophysical Research: Atmospheres 120, 464–479.
- Van Zanten, M., Pons, T., Janssen, J., Voesenek, L., Peeters, A., 2010. On the relevance and control of leaf angle. Critical Reviews in Plant Science 29, 300–316.
- Walker, A.P., Beckerman, A.P., Gu, L., Kattge, J., Cernusak, L.A., Domingues, T.F., Scales, J.C., Wohlfahrt, G., Wullschleger, S.D., Woodward, F.I., 2014. The relationship of leaf photosynthetic traits–V_{cmax} and J_{max}–to leaf nitrogen, leaf phosphorus, and specific leaf area: a meta-analysis and modeling study. Ecology and Evolution 4, 3218–3235.
- Wang, Y., Song, Q., Jaiswal, D., P de Souza, A., Long, S.P., Zhu, X.G., 2017. Development of a three-dimensional ray-tracing model of sugarcane canopy photosynthesis and its application in assessing impacts of varied row spacing. Bioenergy Research 10, 626–634.
- Wang, Y.P., Leuning, R., 1998. A two-leaf model for canopy conductance, photosynthesis and partitioning of available energy I: Model description and comparison with a multi-layered model. Agricultural and Forest Meteorology 91, 89–111.
- Watanabe, T., Hanan, J.S., Room, P.M., Hasegawa, T., Nakagawa, H., Takahashi, W., 2005. Rice morphogenesis and plant architecture: measurement, specification and the reconstruction of structural development by 3D architectural modelling. Annals of Botany 95, 1131–1143.
- Wise, R.R., Frederick, J.R., Alm, D., Kramer, D., Hesketh, J., Crofts, A., Ort, D., 1990. Investigation of the limitations to photosynthesis induced by leaf water deficit in field-grown sunflower (*Helianthus annuus* L.). Plant, Cell & Environment 13, 923–931.
- Yang, X., Li, R., Jablonski, A., Stovall, A., Kim, J., Yi, K., Ma, Y., Beverly, D., Phillips, R., Novick, K., et al., 2023. Leaf angle as a leaf and canopy trait: Rejuvenating its role in ecology with new technology. Ecology Letters 26, 1005–1020.
- Zhuang, J., Chi, Y., Wang, Y., Zhou, L., 2023. Trade-off of leaf-scale resource-use efficiencies along the vertical canopy of the subtropical forest. Journal of Plant Physiology 286, 154004.